

# Photocatalytic behavior of TiO<sub>2</sub> and TiO<sub>2</sub>/CS nanoparticles under UV irradiation

## Comportamiento fotocatalítico de nanopartículas de TiO<sub>2</sub> y TiO<sub>2</sub>/CS bajo irradiación UV

Edgar Mosquera-Vargas <sup>1a, 2</sup>, Daniela Herrera-Molina <sup>1b</sup>, Jesús E. Diosa <sup>1c, 2</sup>

<sup>1</sup> Grupo de Transiciones de Fase y Materiales Funcionales, Departamento de Física, Universidad del Valle, Colombia. Email: [edgar.mosquera@correounivalle.edu.co](mailto:edgar.mosquera@correounivalle.edu.co) <sup>a</sup>, [daniela.herrera@correounivalle.edu.co](mailto:daniela.herrera@correounivalle.edu.co) <sup>b</sup>, [jesus.diosa@correounivalle.edu.co](mailto:jesus.diosa@correounivalle.edu.co) <sup>c</sup>. Orcid: 0000-0003-1561-6994 <sup>a</sup>, 0000-0001-6168-0765 <sup>b</sup>, 0000-0002-1919-1922 <sup>c</sup>

<sup>2</sup> Centro de Excelencia en Nuevos Materiales, Universidad del Valle, Colombia.

Received: 2 June 2022. Accepted: 17 June 2022. Final version: 12 July 2022.

### Abstract

TiO<sub>2</sub> nanoparticles and TiO<sub>2</sub>/CS nanocomposites have been synthesized using the sol-gel method. Characterization by XRD, FTIR, and UV-vis was carried out to determine the structure, size, functional groups, and energy band gap of the synthesized samples. Moreover, the methyl orange (MO) degradation capability of nanoparticles and nanocomposites under ultraviolet light was studied, and the results are described in detail.

**Keywords:** semiconducting nanoparticles; properties; photocatalysis.

### Resumen

Nanopartículas de TiO<sub>2</sub> y nanocompuestos de TiO<sub>2</sub>/CS se han sintetizado mediante el método sol-gel. Se llevó a cabo la caracterización por XRD, FTIR y UV-vis para determinar la estructura, el tamaño, los grupos funcionales y la banda prohibida de energía de los sistemas de muestra. Además, se estudió la capacidad de degradación del anaranjado de metilo (AM) de las nanopartículas y los nanocompuestos bajo luz ultravioleta, y los resultados son descritos en detalle.

**Palabras clave:** nanopartículas semiconductoras; propiedades; fotocatalisis.

### 1. Introduction

During the last decades, metal oxides semiconductors such as titanium dioxide (TiO<sub>2</sub>) has been received attention due to their attractive physical and chemical properties, as well as their interesting properties in optoelectronic devices, sensing, and photocatalytic and photovoltaic applications [1], [2], [3]. Concerning environmental applications (such as photocatalysts), this material depends on its structure and crystalline phase (anatase, rutile, and brookite), dimensions (1D, 2D, and

3D), morphology, and composition (mixed phases) [1], [4]. However, various studies show that many factors influence the photocatalytic activity of TiO<sub>2</sub> under UV-visible illumination, such as particle size, specific surface area, and structure, to name a someone [1], [4].

Furthermore, TiO<sub>2</sub> is inactive material in the visible region due to its wide energy band gap of 3.2 eV, limiting the use of this material in solar photocatalysis. However, Saravanan et. al., [5] reported that mixed TiO<sub>2</sub> will be used in the photodegradation of organics pollutants under

ISSN Printed: 1657 - 4583, ISSN Online: 2145 - 8456.

This work is licensed under a Creative Commons Attribution-NoDerivatives 4.0 License. [CC BY-ND 4.0](https://creativecommons.org/licenses/by-nd/4.0/)



How to cite: E. Mosquera-Vargas, D. Herrera-Molina, J. E. Diosa, "Photocatalytic behavior of TiO<sub>2</sub> and TiO<sub>2</sub>/CS nanoparticles under UV irradiation," *Rev. UIS Ing.*, vol. 21, no. 3, pp. 77-84, 2022, doi: <https://doi.org/10.18273/revuin.v21n3-2022007>.

visible light by lowering their energy band gap. Also, the use of chitosan (CS) is the safest route to carry out visible light degradation due to that contains hydroxyl and amino groups [5]. In addition, the synthesis methods have an important effect on the photocatalytic activity of metal oxide semiconductors [6]. Furthermore, TiO<sub>2</sub> is active under ultraviolet light.

Thus, this work aims is to study the photocatalytic behavior of TiO<sub>2</sub> and CS composites under UV light considering the study reported by Saravanan et. at., [5] of TiO<sub>2</sub>/CS under visible light. Here, TiO<sub>2</sub> nanoparticles and two percentages of TiO<sub>2</sub>/CS nanocomposites have been synthesized and their properties studied. Additionally, the synthesized nanocatalysts were used to degrade methyl orange (MO) dye under UV light.

## 2. Methodology

### 2.1. Materials

For the synthesis of TiO<sub>2</sub> and TiO<sub>2</sub>/CS samples, titanium tetra isopropoxide (TTIP, Purity 97 %, Sigma-Aldrich), Chitosan (CS, medium molecular weight 75 – 85 % deacetylated, Sigma-Aldrich), sodium hydroxide (NaOH, Purity > 99 %, Sigma Aldrich) and acetic acid (CH<sub>3</sub>COOH, Purity > 99 %, J.T. Baker) were used without further purification. Methyl orange (MO, Purity ≥ 97.0 %) was purchased from PanReac AppliChem and used for evaluating the photocatalytic capabilities of the samples. All solutions used in the experiments were prepared with deionized water.

### 2.2. Synthesis of TiO<sub>2</sub> nanoparticles

A sol-gel method was employed to synthesize TiO<sub>2</sub> nanocatalyst. The synthesis was made by the hydrolysis-condensation of TTIP using acetic acid as a solvent agent. First, a solution of acetic acid and deionized water (2% v/v) was prepared. Then, TTIP (at 5 % v/v) as a precursor agent was added until obtaining a homogeneous solution. The homogeneous solution was sonicated for 3 h and then dried on a stirrer hot plate until obtaining the gel formation. After that, the sol-gel product was ground in a mortar to obtain fine powder for analysis. The powder was calcined in a muffle at different temperatures (400, 450, and 500 °C) for 3 h to obtain the TiO<sub>2</sub> anatase phase. A yellow-white fine powder was obtained.

### 2.3. Synthesis of TiO<sub>2</sub>/CS nanocomposites

For the preparation of TiO<sub>2</sub>/CS nanocomposite, the sample calcined at 450 °C was used. This sample exhibit an absorption peak in the UV-vis spectrum closer to the visible range in comparison to the other powders. The

proportions TiO<sub>2</sub>/CS (w/w) of 95/5 and 80/20 were studied. After that, with these two proportions, two solutions of 2 % w/v were prepared using acetic acid as solvent. Then, the samples were placed on a magnetic hot plate stirring for 30 min. Sodium hydroxide solved in water at a 50 % concentration was gradually added to the previous solution to control the pH level until it is precipitated. This pH has a value of approximately 6 and 10 for each TiO<sub>2</sub>/CS proportion. Both solutions were taken to the centrifuge for 10 min to separate the liquid phase from the solid. Later, the samples were dryers in an oven at 55 °C for 12 h. The product obtained is macerated to a fine powder.

### 2.4. Characterization

The structural phase and crystallinity of the samples were determined using an X'Pert-PRO of the PANalytical brand, with a CuK<sub>α</sub> radiation ( $\lambda = 0.154$  nm) at room temperature (RT). The XRD was operated at 45 kV. The measurements were done with a step of 0.002°, in 2 $\theta$  angle of 10° to 90°. An FTIR spectrophotometer (model IRAffinity-1 from Shimadzu) in transmittance mode was used to obtain the IR spectra of the samples. UV-vis spectra were recorded at room temperature in the range of 200-800 nm by employing a Double Beam UV-vis spectrophotometer (E-Chrom Tech) with a step of 0.5 nm, respectively. The optical energy band gap ( $E_g$ ) was determined using the Tau plot method through UV-vis measurements. Thermal analyses were carried out using a calorimeter DSC, Q-100, from TA Instrument Brand. The measurement was done in an aluminum capsule (mass: 5 mg) with a ramp of 10 °C/min.

### 2.5. Photocatalysis measurements

Photocatalytic activity experiments were conducted in a homemade photoreactor with a UV lamp. Methyl orange (MO, purity ≥ 97 % from Sigma-Aldrich) was selected to evaluate the photocatalytic capabilities of the samples. This was selected because, unlike methylene blue, it does not degrade under UV irradiation in the absence of a photocatalyst material. A calibration curve was made using MO in deionized water in a concentration between 1 ppm and 10 ppm, using the Double Beam UV-vis spectrophotometer (E-Chrom Tech). Measurements were made using two quartz cell (10 mm x 10 mm). The first one is filled with deionized water as a reference and the second is filled with the sample. All measurements were made with a fixed initial concentration of 5 ppm for the MO in deionized water and the photocatalyst material (TiO<sub>2</sub> nanoparticles and TiO<sub>2</sub>/CS nanocomposites) was added at a concentration of 1 g/L in a beaker. This mixture was placed in the photoreactor under magnetic

stirring for 30 min without light to ensure adsorption/desorption equilibrium, and then under UV irradiation for 4 h. Absorbance measurements were made in this time frame, removing a part of the sample (~ 3 ml) and putting it to centrifuge for 4 min at 3000 rpm to separate the dye solution from photocatalyst material. This procedure was made for each sample. In addition, a calibration plot based on the Beer-Lambert law was established by relating the absorbance to the concentration, and the percentage of MO degradation was calculated using the expression  $\% \eta = \frac{(C_0 - C)}{C_0} \times 100 \%$  [7], where  $C_0$  is the initial concentration and  $C$  is the concentration of MO under UV light.

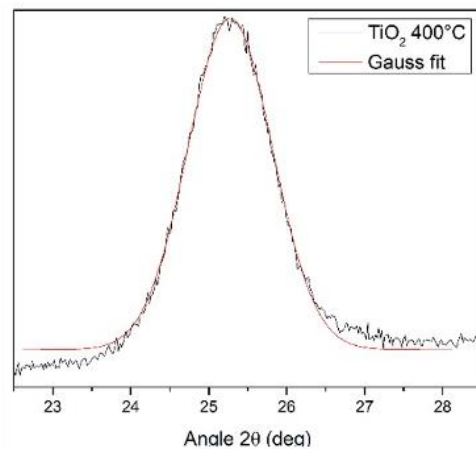
### 3. Results and discussions

Figure 1 shows the principal (101) plane of XRD patterns of the synthesized TiO<sub>2</sub> nanoparticles (NPs) treated at 400, 450, and 500 °C. The patterns have been indexed for the JCPDS 89-4921 reported in Ref [4], with crystal structure corresponding to the tetragonal anatase phase. The crystallite size estimation was determined using Scherrer's formula reported in Ref [7]. Here, the (101) plane was fitted by a Gaussian function to determine the 2θ peak and the line broadening β (FWHM) of the NPs. The results are reported in Table 1. As can be seen, the crystallite size increase with increasing the temperature of synthesis.

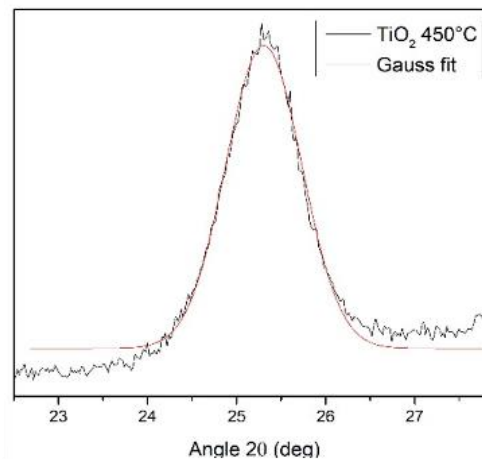
On the other hand, CS shows two principal peaks at around 11° and 21°, which is in agreement with previous reports [5], [8], while TiO<sub>2</sub> NPs exhibit peaks at 2θ values 25.5°, 38.2°, 48.2°, 54°, 55.2°, 62.8°, 69°, 70.6°, and 75.5° and Miller's indexes (101), (004), (200), (105), (211), (204), (116), (220), and (215), respectively. However, the XRD pattern of the anatase phase in the TiO<sub>2</sub>/CS nanocomposite was identical to that of TiO<sub>2</sub> NPs without alteration of its structure (see Figure 2) and confirm the formation of the nanocomposite. Similar results were obtained for the nanocomposites with TiO<sub>2</sub> treated at 400 and 500 °C (not shown).

Table 1. Crystallite size of TiO<sub>2</sub> NPs

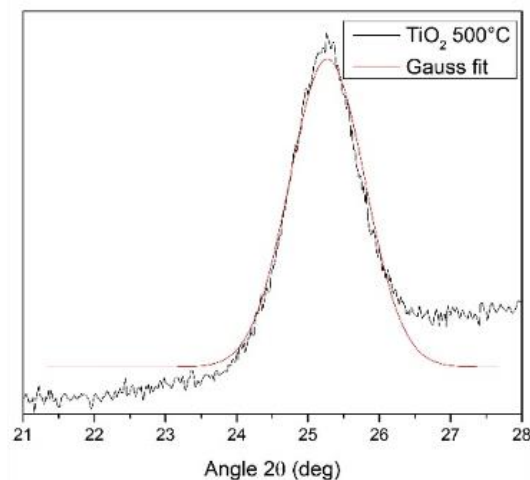
Sample	$\theta_B$ (deg)	$B$ (rad)	Crystallite size, $D$ (nm)
TiO <sub>2</sub> at 400 °C	25.2	0.021	7.3
TiO <sub>2</sub> at 450 °C	25.3	0.017	8.7
TiO <sub>2</sub> at 500 °C	25.2	0.017	8.8



(a)



(b)



(c)

Figure 1. (101) Gauss fit of anatase phase for TiO<sub>2</sub> NPs treated at a) 400 °C, b) 450 °C, and c) 500 °C.

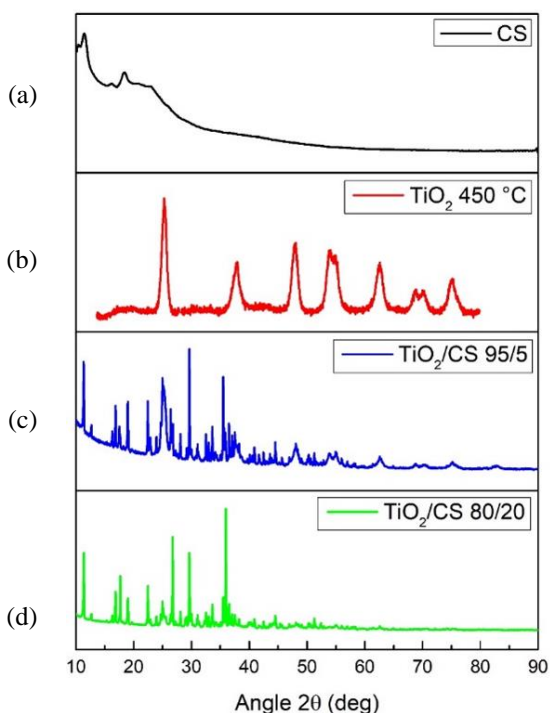


Figure 2. XRD pattern of samples a) CS, b)  $\text{TiO}_2$  NPs, c)  $\text{TiO}_2/\text{CS}$  95/5, and d)  $\text{TiO}_2/\text{CS}$  80/20 treated at  $450^\circ\text{C}$

Figure 3 shows the FTIR spectra for the  $\text{TiO}_2$  NPs treated at  $450^\circ\text{C}$ , chitosan (CS), and nanocomposites. It is clearly observed in all of them that the characteristic stretching mode between  $600$  and  $700\text{ cm}^{-1}$  corresponds to Ti-O-Ti bonds [5]. In the case of the pure CS spectrum, the OH bond is found around  $3342\text{ cm}^{-1}$ . Another functional group is around  $1028\text{ cm}^{-1}$  which is associated with C-O group [8], [9]. Moreover, chitosan contains an amino group that was presented around  $1650\text{ cm}^{-1}$ . The C-H groups may be associated with the band around  $2857\text{ cm}^{-1}$  [9], [10]. After the addition of the  $\text{TiO}_2$  NPs to the chitosan, the stretching vibration of C-O, amino, and hydroxyl groups are modified due to the presence of  $\text{TiO}_2$  NPs. This observation is evidence of the formation of  $\text{TiO}_2/\text{CS}$  system and agrees with XRD results.

Absorbance measurements as a function of radiation's wavelength were carried out to determine the optical energy bandgap ( $E_g$ ) of the samples (not shown) and reported in Table 2. However, the direct and indirect transitions were calculated through Tauc's plot method [4], based on the dependence of the absorption coefficient,  $\alpha$  ( $\alpha = 0$ ), and the photon energy,  $h\nu$ . Here, it was observed that  $\text{TiO}_2$  NPs show an absorbance peak in the UV range. For the  $\text{TiO}_2/\text{CS}$  (80/20 and 95/5) nanocomposites compared with pure  $\text{TiO}_2$ , the  $E_g$  increases for  $\text{TiO}_2/\text{CS}$  95/5 but decreases for  $\text{TiO}_2/\text{CS}$  80/20, see Table 2. In addition, we observed that the

optical absorption edge for direct transition in the anatase phase of  $\text{TiO}_2$  NPs is  $E_g \sim 3.2\text{ eV}$  (387 nm), however, the synthesized NPs exhibit blue shift concerning the bulk reported [4]. Given these results and under UV light, the photocatalytic activity was carried out.

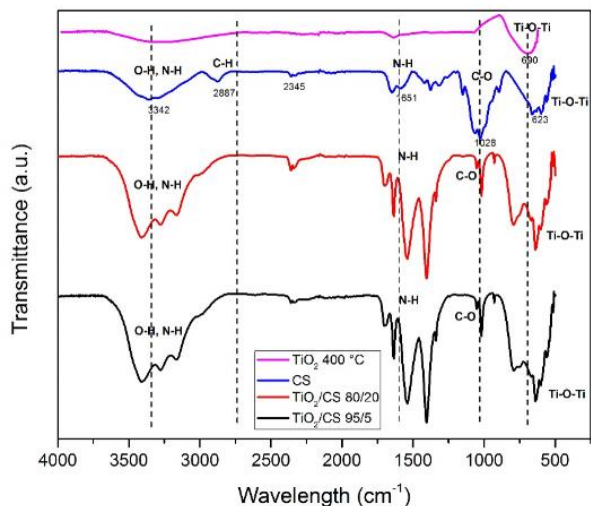


Figure 3. FTIR spectra of samples studied

Table 2. Optical energy bandgap of synthesized samples

Sample	Optical $E_g$ (eV) indirect transition	Optical $E_g$ (eV) direct transition
$\text{TiO}_2$ at $400^\circ\text{C}$	4.11	3.75
$\text{TiO}_2$ at $450^\circ\text{C}$	4.13	3.74
$\text{TiO}_2$ at $500^\circ\text{C}$	4.11	3.75
$\text{TiO}_2/\text{CS}$ 95/5	4.19	3.89
$\text{TiO}_2/\text{CS}$ 80/20	3.37	2.62

A differential scanning calorimetry (DSC) study was carried out to determine thermal events associated with phase transition in the samples. All NPs, do not show any thermal phase transition in the range from  $-50$  to  $550^\circ\text{C}$ . however, for the  $\text{TiO}_2/\text{CS}$  nanocomposites (See Figure 4), several endothermic and exothermic transitions are observed. One of them, at about  $450^\circ\text{C}$ , which is an exothermic transition is associated with the CS decomposition of the amine group, which for pure CS occurs at around  $300^\circ\text{C}$ . therefore, the results indicate that the addition of  $\text{TiO}_2$  NPs to CS stabilizes the CS polymer matrix.

On the other hand, the nanocomposite sample,  $\text{TiO}_2/\text{CS}$  95/5, shows an exothermic peak at about  $-50^\circ\text{C}$  that may be associated with a spontaneous recrystallization process followed by its melting point at  $\sim 60^\circ\text{C}$ . There is another endothermic peak at around  $150^\circ\text{C}$  that may be

attributed to the evaporation of water molecules trapped in the TiO<sub>2</sub> NPs. These phenomena, which are not frequently observed, were not exhibited by the 80/20 concentration sample, probably due to a different thermal history or amorphous character. Finally, an endothermic peak around 330 °C is observed in both TiO<sub>2</sub>/CS samples, which can be attributed to melting of a crystalline phase in the nanocomposites due to the presence of TiO<sub>2</sub> in CS.

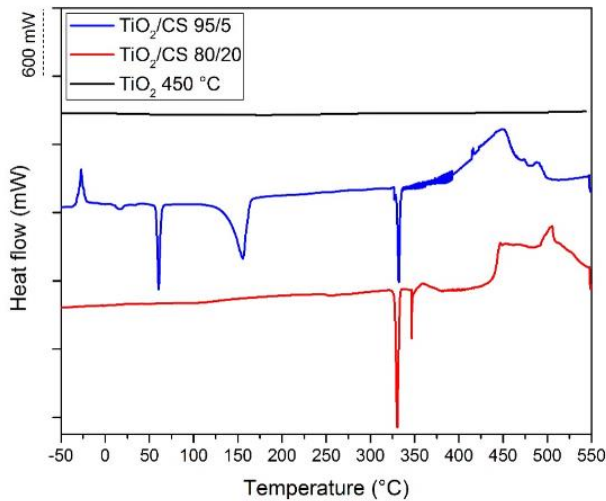
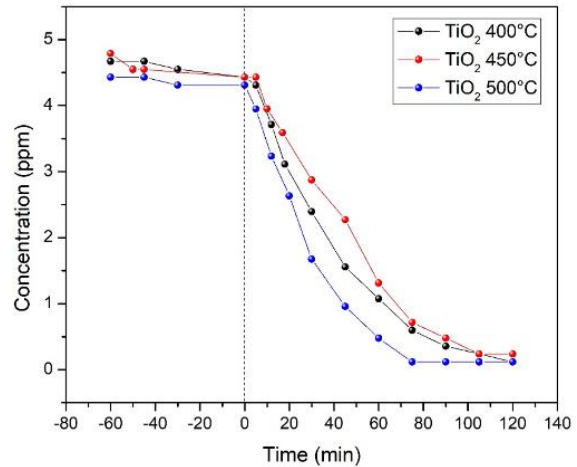


Figure 4. DSC of samples studied

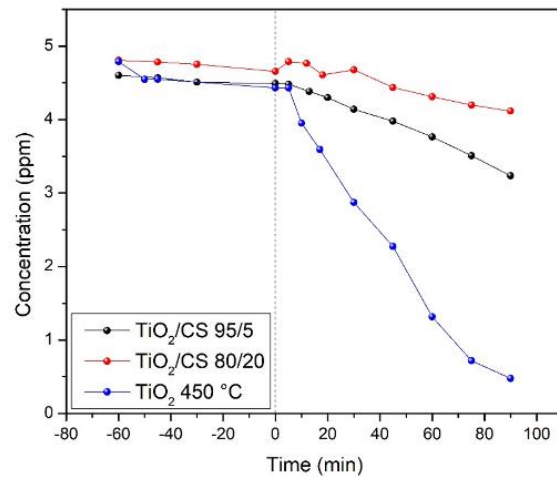
The main objective of this work is to evaluate the degradation capacity of the synthesized nanocomposite system under ultraviolet light. As mentioned in the experimental section, methyl orange (MO) dye was used as the contaminating organic molecule. Making use of a photoreactor, the radiation inside the sample was controlled. Initially, a photolysis investigation (without catalyst) was performed, and its results showed that the MO dye had good stability under ultraviolet illumination. First without illumination and then with light, the irradiated dye solutions were collected in a vial at different periods. The absorption value of the solutions was measured using a UV-Vis spectrophotometer. However, qualitatively is observed that the TiO<sub>2</sub> NPs are the best photocatalyst under UV light with a degradation time of between 75 to 90 min. Instead, in the nanocomposites, the degradation process was slower than in TiO<sub>2</sub> NPs.

To obtain a quantitative analysis of the photocatalytic activity of the samples, degradation kinetics studies were carried out. First, a calibration curve of MO was done to know the concentration as a function of absorbance.

Then, the photodegradation was made for each sample. It was observed that TiO<sub>2</sub> NPs acts as a good catalyst for MO degradation under UV light. The results are shown in Figure 5.



(a)

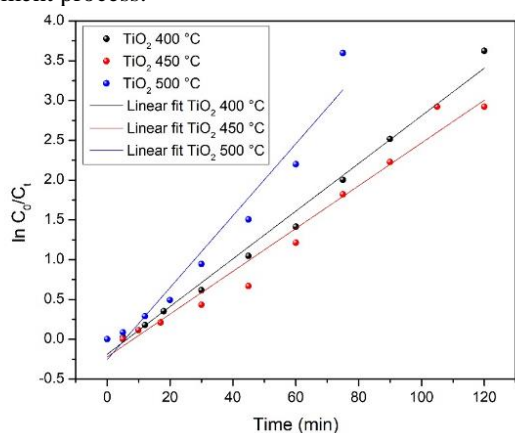


(b)

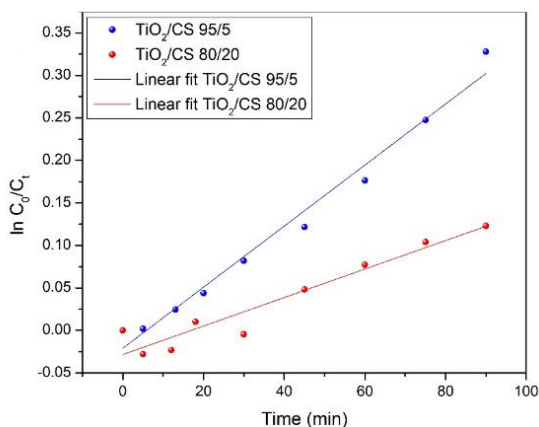
Figure 5. Degradation Kinetic for samples studied. a) nanoparticles, and b) nanocomposites

Additionally, a plot  $\ln\left(\frac{C_0}{C}\right)$  as a function of the time of UV light exposure was made to obtain the rate constant  $k$  of degradation. This constant determines how fast the reaction occurs, such that, higher values of  $k$  correspond to faster reactions. By fitting the linear part of the curves, the corresponding slopes (or  $k$  values) are determined and reported in Figure 6 and Table 3. Here, the TiO<sub>2</sub>/CS system was less efficient than TiO<sub>2</sub> NPs where the worse photocatalytic material under UV radiation was TiO<sub>2</sub>/CS 80/20.

Here, there is low recombination of the reactive hole ( $h^+$ ) and electron ( $e^-$ ) pair in the nanocomposite systems, which is required for the photocatalytic reactions under UV-visible illumination. In addition, during the adsorption and degradation process MO adsorbed on the surface of the catalyst affects the recombination process during the photocatalytic activity under UV light. The results of this study can contribute to the dye wastewater treatment process.



(a)



(b)

Figure 6. Linear fit of  $\ln\left(\frac{C_0}{C_t}\right)$  as a function of exposure time of the samples studied. a) nanoparticles, and b) nanocomposites

Table 3. Degradation rate constant for each sample of a MO dye solution

Sample	Rate constant $k$ ( $\text{min}^{-1}$ )
TiO <sub>2</sub> at 400 °C	0.0299
TiO <sub>2</sub> at 450 °C	0.0268
TiO <sub>2</sub> at 500 °C	0.0451
TiO <sub>2</sub> /CS 95/5	0.0036
TiO <sub>2</sub> /CS 80/20	0.0017

#### 4. Conclusions

TiO<sub>2</sub> nanoparticles and TiO<sub>2</sub>/CS nanocomposites were synthesized by the sol-gel method to perform adsorption-photocatalytic decolorization of MO dye under UV irradiation. XRD and FTIR results confirm the structure of the nanoparticles and nanocomposite using chitosan as the induced matrix. The crystallite size and optical energy bandgap of the samples were determined. All nanoparticles were photoactive for MO degradation after 75 min of being irradiated with UV light. Instead, the nanocomposites present lower photocatalytic activity due to poor recombination of hole-electron pairs under UV light. The results of this study may be useful in the dye wastewater treatment process.

#### Acknowledgment and Funding Statement

This work has been supported by *Universidad del Valle* – Colombia (Strengthening of Centers and Institutes) and the Colombian Government (Minciencias, BPIN 2021000100424).

#### Declaration of Competing Interest

The authors declare that they have no known competing financial interests or personal relationships that could have appeared to influence the work reports in this manuscript.

#### References

- [1] M. Rosales, T. Zoltan, C. Yadarola, E. Mosquera, F. Gracia, A. García, "The influence of the morphology of 1D TiO<sub>2</sub> nanostructures on photogeneration of reactive oxygen species and enhanced photocatalytic activity," *J. Mol. Liq.*, vol. 281, 59-69, 2019, doi: <https://doi.org/10.1016/j.molliq.2019.02.070>
- [2] H. Liu, L. Gao, "Preparation and properties of nanocrystalline alpha-Fe<sub>2</sub>O<sub>3</sub>-sensitized TiO<sub>2</sub> nanosheets as a visible light photocatalyst," *J. Am. Ceram. Sc.*, vol 89, 370-373, 2006, doi: <https://doi.org/10.1111/j.1551-2916.2005.00686.x>
- [3] M.A. Vargas-Urbano, L. Marín, W. M. Castillo, L. A. Rodríguez, C. Magén, M. Manotas-Albor, J. E. Diosa, K. Gross, "Effect of ethylene glycol: citric acid molar ratio and pH on the morphology, vibrational, optical and electronic properties of TiO<sub>2</sub> and CuO powders synthesized by Pehini method," *Preprints*, 2022, doi: <https://doi.org/10.20944/preprints202205.0150.v1>

[4] E. Mosquera-Vargas, D. Herrera-Molina, J. E. Diosa, “Structural and optical properties of TiO<sub>2</sub> nanoparticles and their photocatalytic behavior under visible light”, *Ing. Competitividad*, 23 vol. 2, e21310965, 2021, doi: <https://doi.org/10.25100/iyv.v23i2.10965>

[5] R. Saravanan, J. Aviles, F. Gracia, E. Mosquera, V.K. Gupta, “Crystallinity and lowering band gap induced visible light photocatalytic activity of TiO<sub>2</sub>/CS (chitosan) nanocomposites,” *Int. J. Biol. Macromol.*, vol 109, pp. 1239-1245, 2018, doi: <https://doi.org/10.1016/j.ijbiomac.2017.11.125>

[6] Y. Quintero, E. Mosquera, J. Diosa, A. García, “Ultrasonic-assisted sol-gel synthesis of TiO<sub>2</sub> nanostructures: Influence of synthesis parameters on morphology, crystallinity, and photocatalytic performance,” *J. Sol-Gel Sci. Technol.*, vol. 94, pp. 477-485, 2020, doi: <https://doi.org/10.1007/s10971-020-05263-6>

[7] M. A. Vargas, E. M. Rivera-Muñoz, J. E. Diosa, E. E. Mosquera, J. E. Rodríguez-Páez, “Nanoparticles of ZnO and Mg-doped ZnO: Synthesis, characterization and efficient removal of methyl orange (MO) from aqueous solution,” *Ceram Intern.*, vol. 47, pp. 15668-15681, 2021, doi: <https://doi.org/10.1016/j.ceramint.2021.02.137>

[8] H. Zhu, R. Jiang, Y. Fu, Y. Guan, J. Yao, L. Xiao, G. Zeng, “Effective photocatalytic decolorization of methyl orange utilizing TiO<sub>2</sub>/ZnO/chitosan nanocomposite films under simulated solar irradiation,” *Desalination*, vol. 286, pp. 41–48, 2012, doi: <https://doi.org/10.1016/j.desal.2011.10.036>

[9] M.A. Nawi, A.H. Jawad, S. Sabar, W.S.W. Ngah, “Immobilized bilayer of TiO<sub>2</sub>/Chitosan system for the removal of phenol under irradiation by a 45 watt compact fluorescent lamp”, *Desalination*, vol. 280, pp. 288–296, 2011, doi: <https://doi.org/10.1016/j.desal.2011.07.013>

[10] Q. Li, H. Su, T. Tan, “Synthesis of ion-imprinted chitosan-TiO<sub>2</sub> adsorbent and its multi-functional performances,” *Biochem. Eng. J.*, vol. 38, pp. 212–218, 2008, doi: <https://doi.org/10.1016/j.bej.2007.07.007>